MULTIPLE TRANSITIONS IN VACUUM DARK ENERGY AND H_0 TENSION

Hossein Mos'hafi

School of Astronomy, IPM

This talk is based on paper: ***Astrophys.J.* 940 (2022) 2, 121**

H. Moshafi, H. Firouzjahi, A. Talebian

STANDARD MODEL OF COSMOLOGY

- A singularity at the beginning
- Two unknown main components:
  - Dark Energy (Λ ?)
  - Dark Matter (CDM ?)

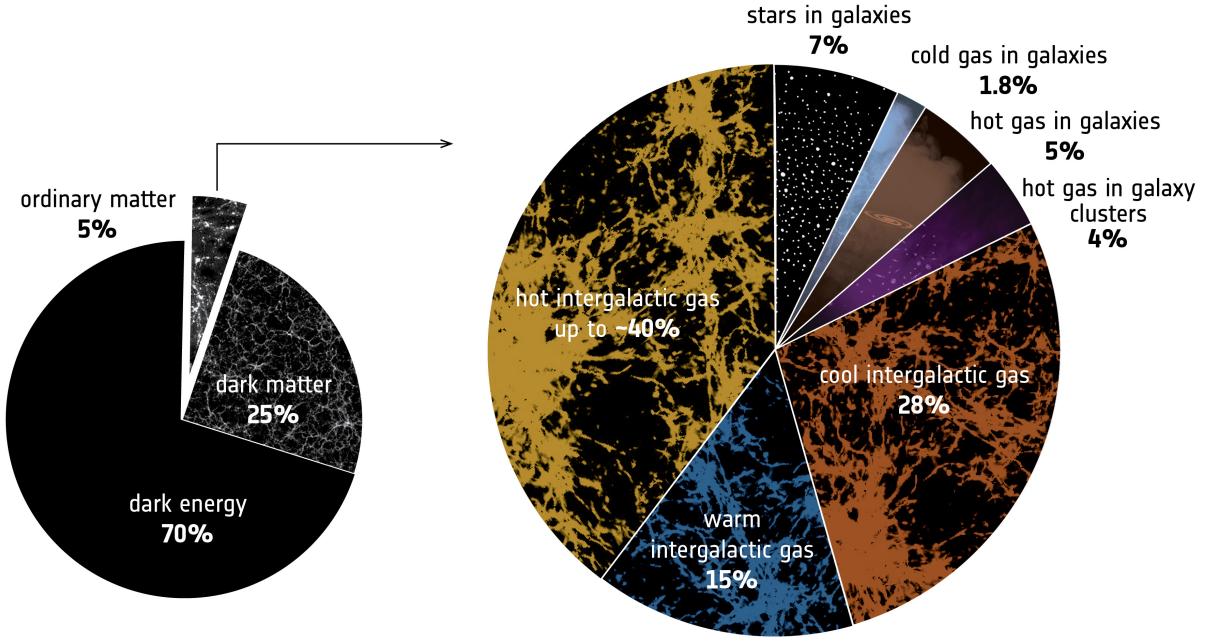

CHALLENGES TO THE STANDARD MODEL OF COSMOLOGY

- In the standard LCDM model we assume ingredients take on their simplest (Vanilla) form
- The Planck experiment has measured the CMB power spectra with an exquisite precision, but the constraints for the cosmological parameters are always model-dependent.
- Over the last decade cosmological observations have significantly improved, both for early-time as well as late-time observations.
- In principle, scales measured at different times should appear consistent when interpreted in the context of an accurate, time-dependent cosmological model.

CHALLENGES TO THE STANDARD MODEL OF COSMOLOGY

- S_8 tension
- A_{lens} tension
- H_0 tension
- …

S_8 TENSION

- A significant tension between Planck data with redshift surveys data and weak lensing measurements has been reported, about the Ω_m, and the amplitude of growth of the structures, σ_8, also quantified in terms of the parameter: $S_8 = \sigma_8\sqrt{\frac{\Omega_m}{0.3}}$.
- A higher S_8value is estimated from CMB data assuming LCDM model, namely, $S_8 = 0.834 \pm 0.016$ from Planck data.
- This tension is above the 2σ level with KiDS-450 ($S_8 = 0.745 \pm 0.039$), KiDS+VIKING-450 ($S_8 = 0.737^{+0.040}_{-0.036}$) and DES ($S_8 = 0.738 \pm 0.021$).
- The KiDS-1000 team reported a 3σ tension with Planck-CMB.
- The tension becomes 3.2σ if we consider the combination of VIKING-450 and DESY1 and 3.4σ for BOSS+VIKING-450 .

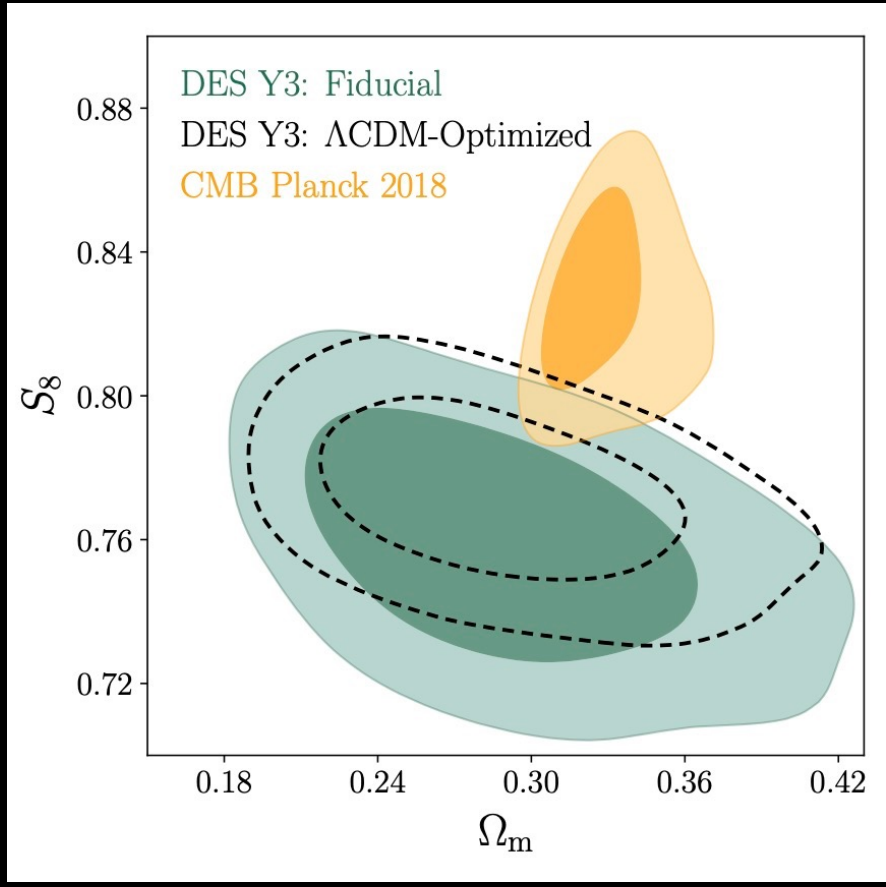

THE A_{Lens} ANOMALY

- The lensing magnifies the angular size of the primordial fluctuations in some places on the sky and de-magnifies others.
- The acoustic peaks are reduced slightly, and the troughs between them filled in.
- When the theoretical prediction for this smoothing is compared with the Planck data, it is found that the lensing smoothing is larger than expected by roughly 10%.
- The A_{Lens} anomaly is persistent with a value $A_{Lens} = 1.149 \pm 0.072$, that constitute 2σ tension with LCDM cosmology.

WHAT IS HUBBLE CONSTANT?

The Hubble constant (H_0) describes the expansion rate of the Universe today.

$$H \equiv \frac{\dot{a}}{a}$$

Hubble-Lemaître law

$$1 + z = \frac{\lambda_{obs}}{\lambda_{emit}} \leftarrow \quad v = H_0 d \quad \leftarrow$$

Spectrometry
photometry

Standard candles, standard rulers, standard sirens

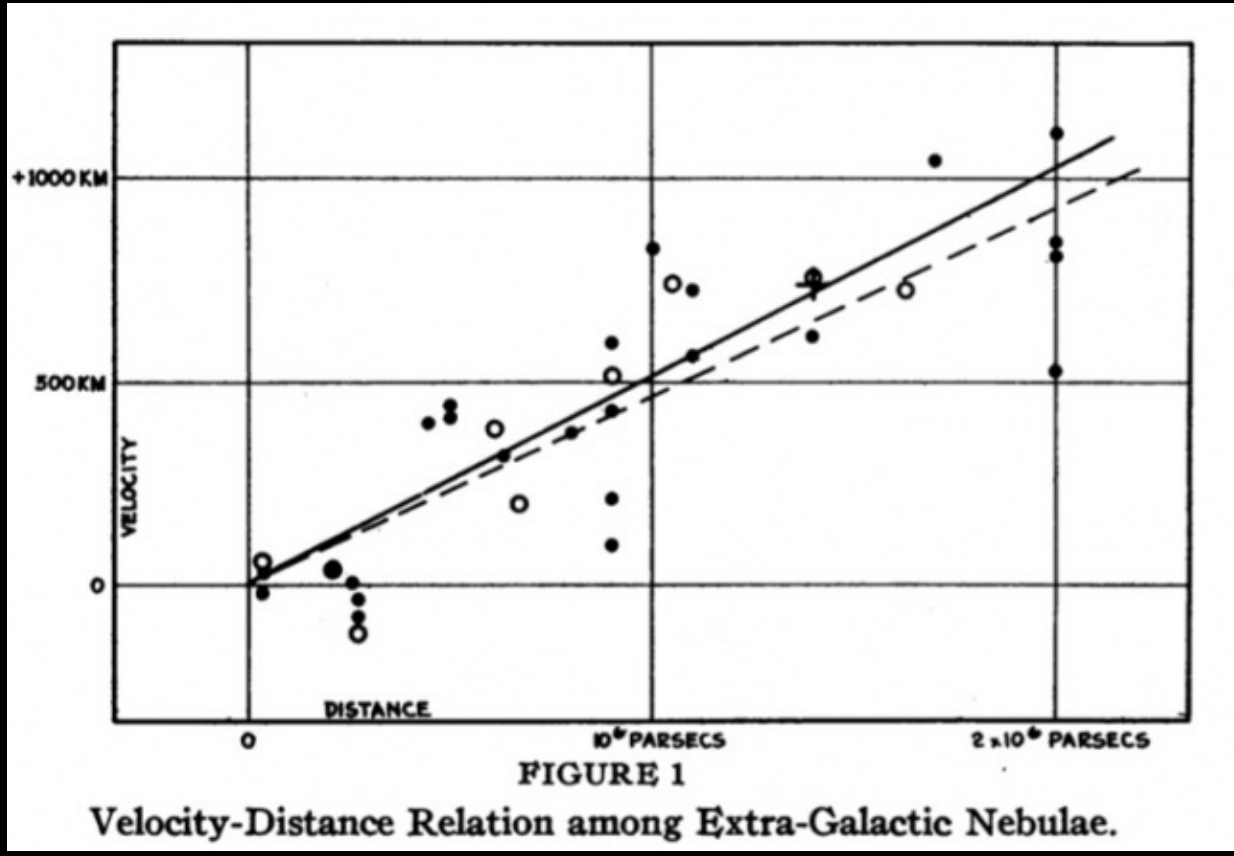

FIGURE 1

Velocity-Distance Relation among Extra-Galactic Nebulae.

H IS NOT A CONSTANT

$$\left(\frac{\dot{a}}{a}\right)^2 \equiv H^2(z) = H_0^2[\Omega_r(1+z)^4 + \Omega_m(1+z)^3 + \Omega_k(1+z)^2 + \Omega_{\mathrm{DE}}]$$

$$H \equiv \frac{\dot{a}}{a} \qquad d_L(z) = (1+z)\int_0^z \frac{cdz'}{H(z')}$$

$$d_A(z) = \frac{1}{(1+z)}\int_0^z \frac{cdz'}{H(z')}$$

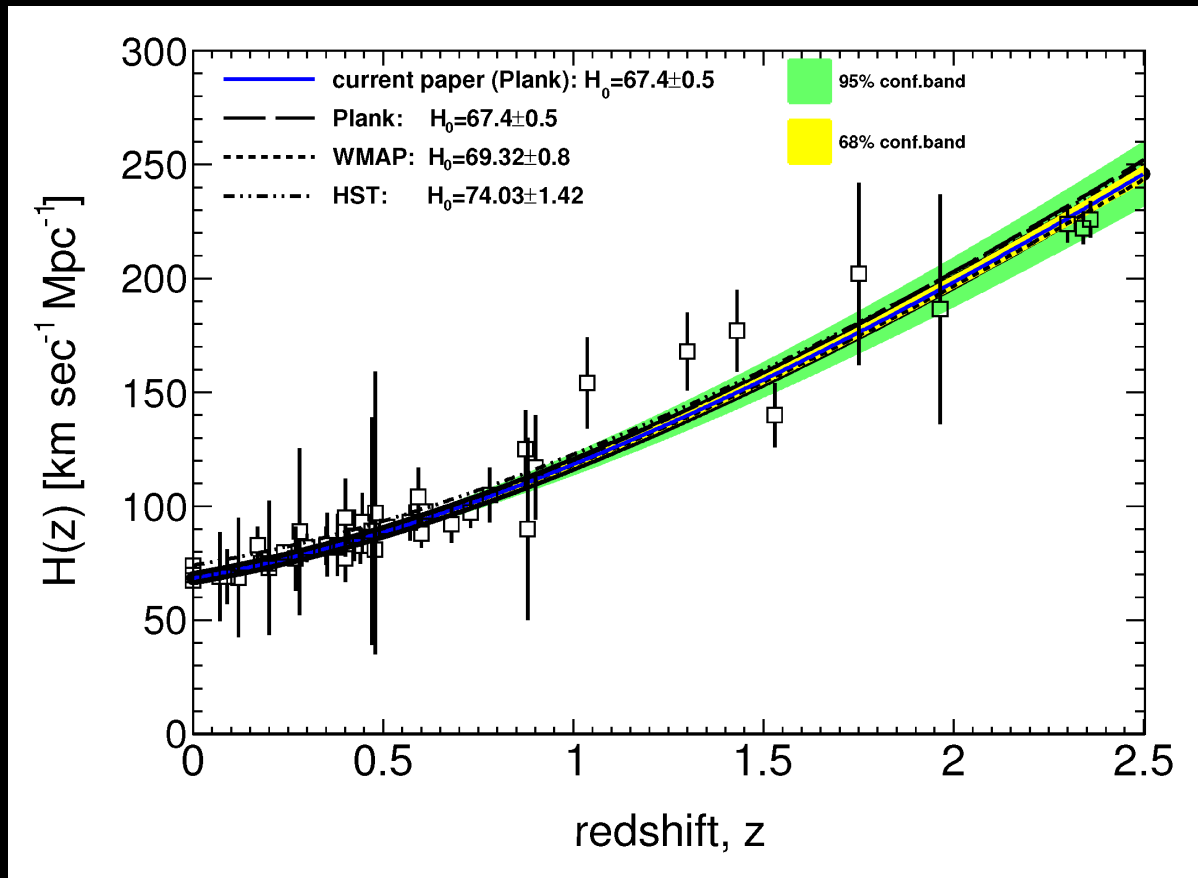

TWO MAIN METHODS TO MEASURE H_0

- Late-time Universe, direct measurements
- Early-time Universe, indirect measurement

LATE-TIME UNIVERSE, DIRECT MEASUREMENT

- Measuring the distance and the recessional velocity of standard candles, and computing the proportionality factor.

- This approach is model independent and based on geometrical measurements.

$$d_L(z) = (1+z)\int_0^z \frac{c dz'}{H(z')}$$

$$d_A(z) = \frac{1}{(1+z)}\int_0^z \frac{c dz'}{H(z')}$$

EARLY-TIME UNIVERSE, INDIRECT MEASUREMENT

- Considering early universe measurements, and assuming a model for the expansion history of the universe.
- Main observation is the CMB anisotropies and is model-dependent

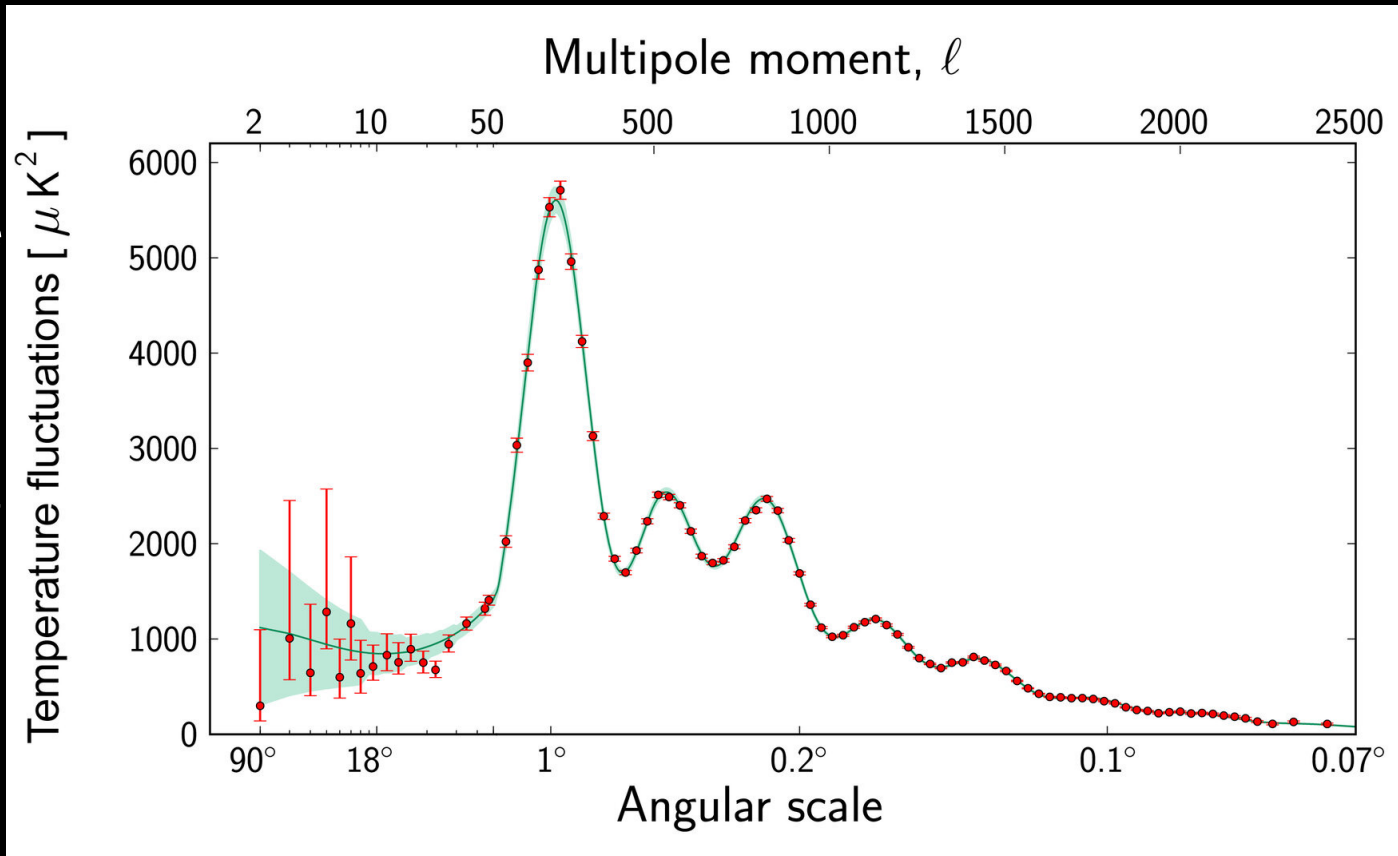

EARLY-TIME UNIVERSE, INDIRECT MEASUREMENT

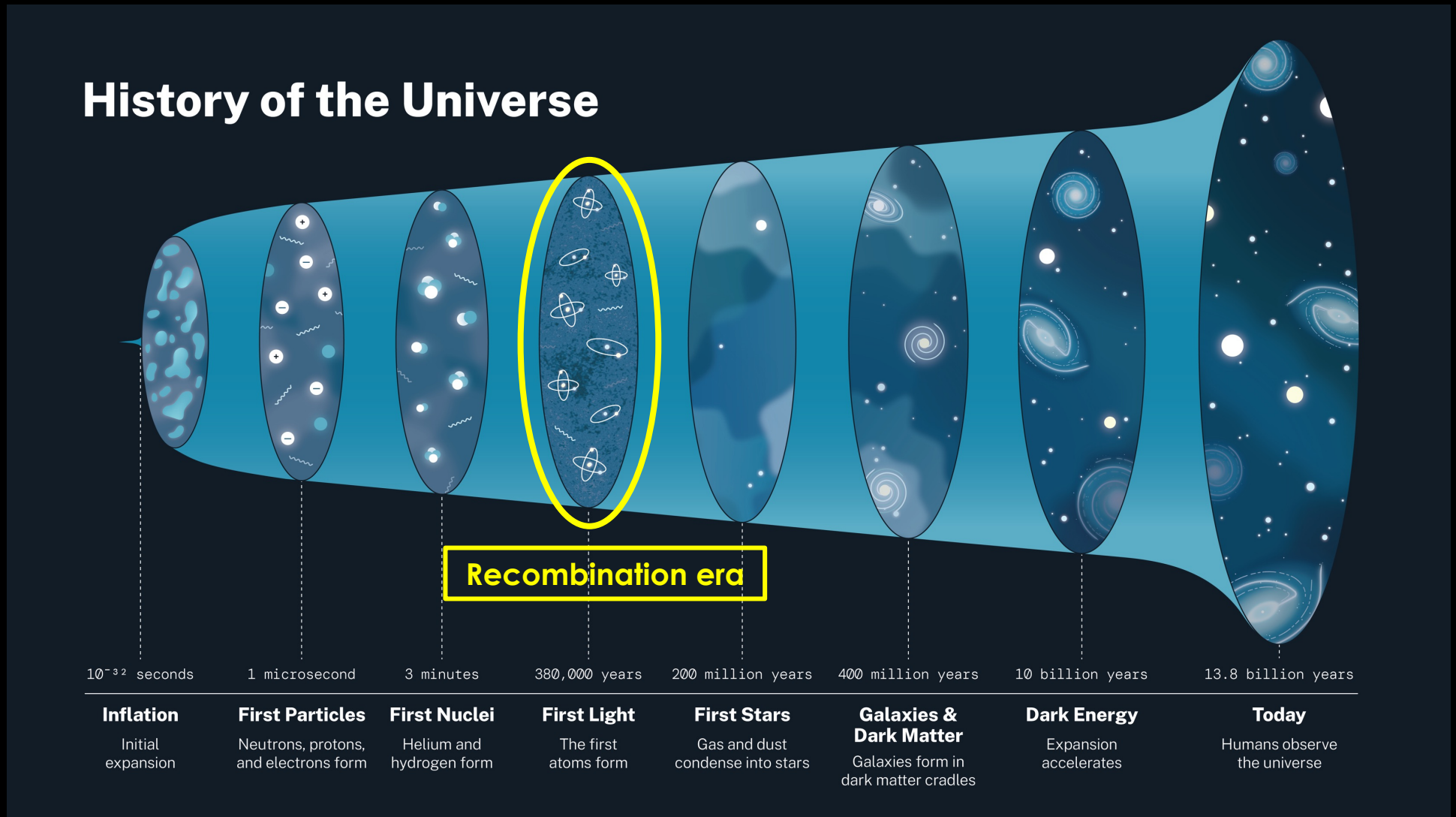

EARLY-TIME UNIVERSE, INDIRECT MEASUREMENT

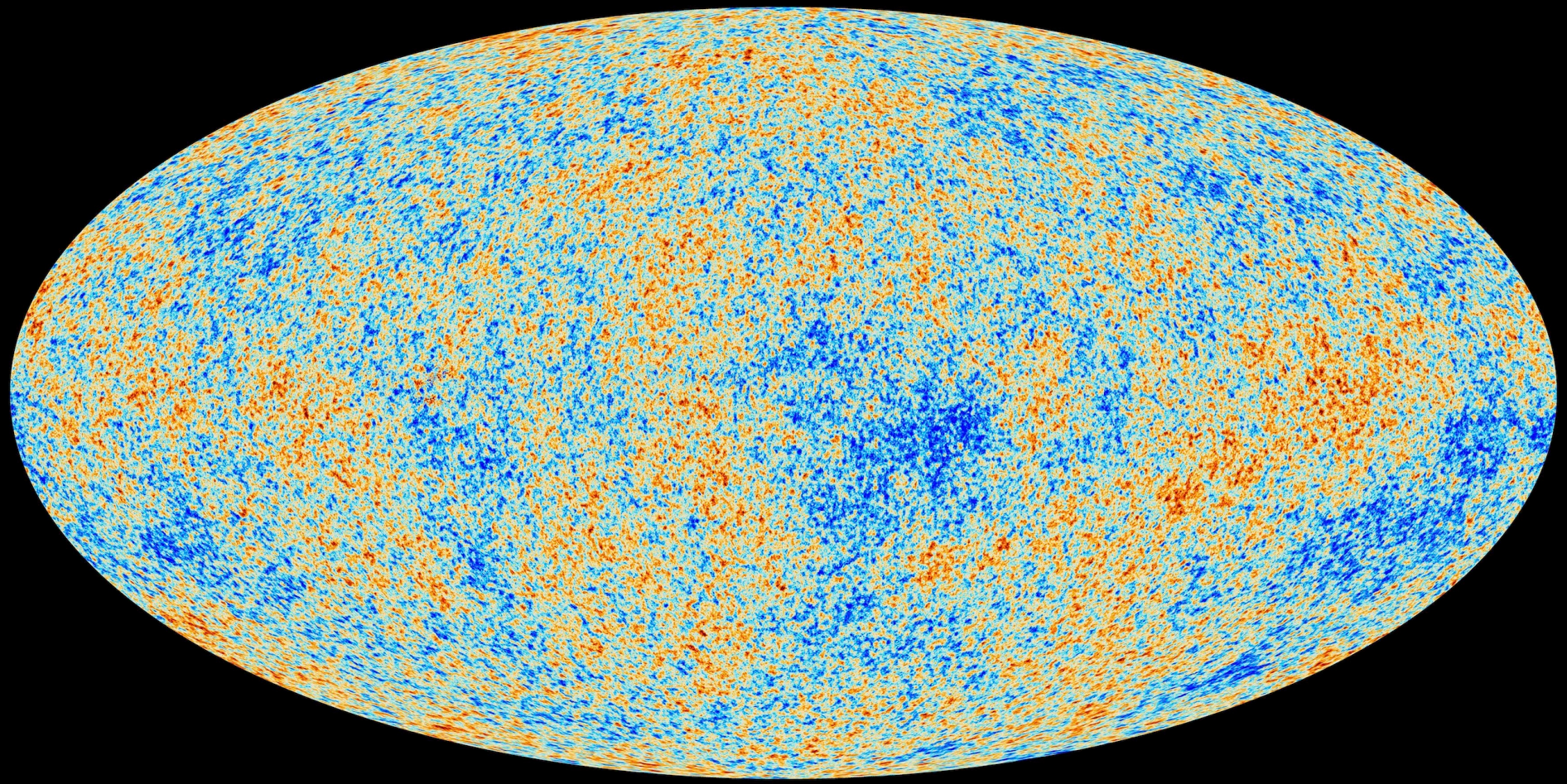

EARLY-TIME UNIVERSE, INDIRECT MEASUREMENT

By fitting to the CMB spectrum, one constrains all parameters of the ΛCDM model, including H_0

$$\boldsymbol{P = \{\Omega_b h^2, \Omega_{cdm} h^2, \tau_{re}, 1000\Theta_{MC}, A_s, n_s\}}$$

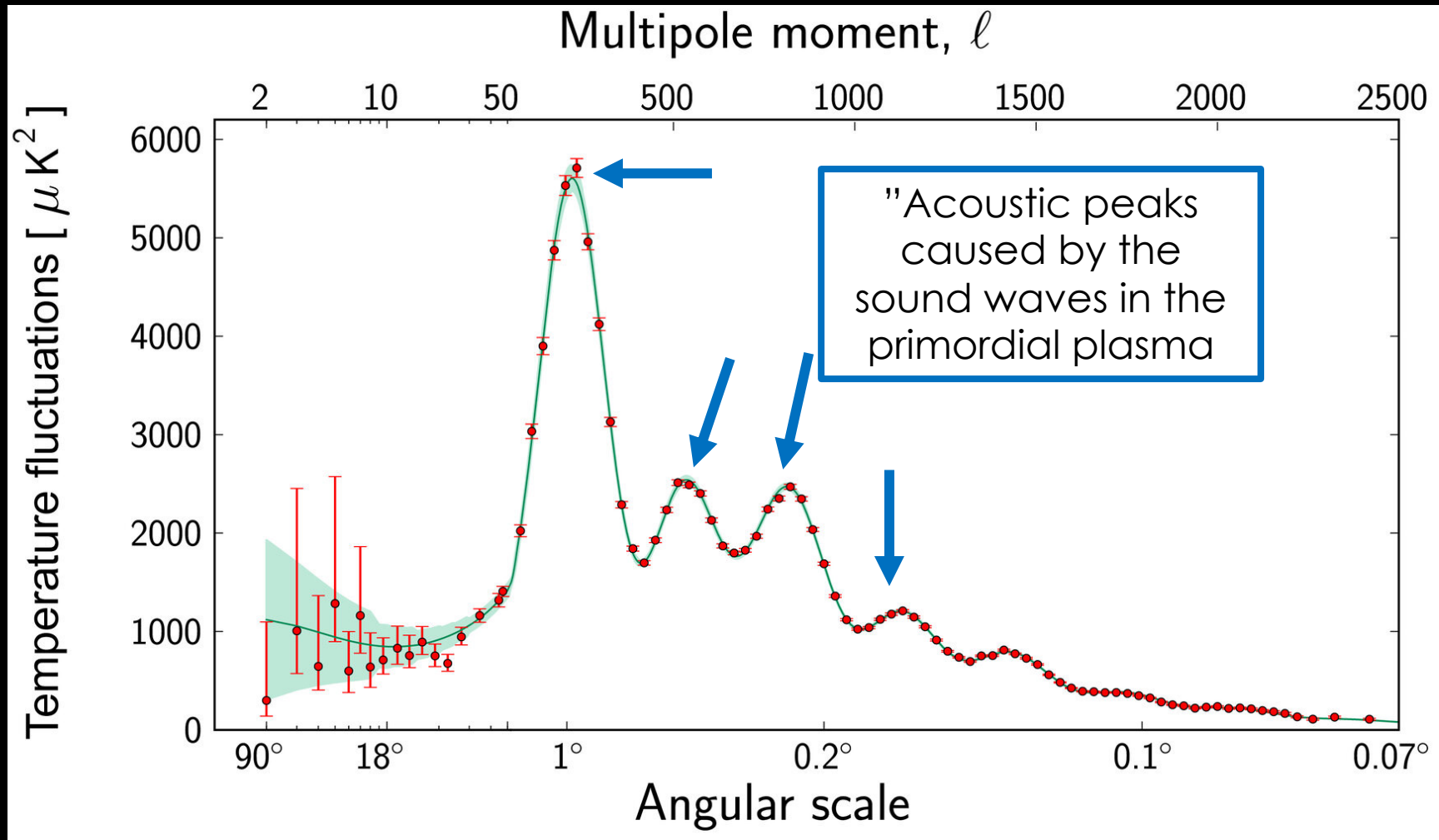

HOW DOES CMB CONSTRAIN H_0 ?

- Positions of the acoustic peaks tell us the angular size of the sound horizon at recombination, $\theta_* = \frac{r_s}{r_*}$
- A smaller sound horizon r_s would imply a shorter distance to the redshift of recombination r_*, implying a larger H_0

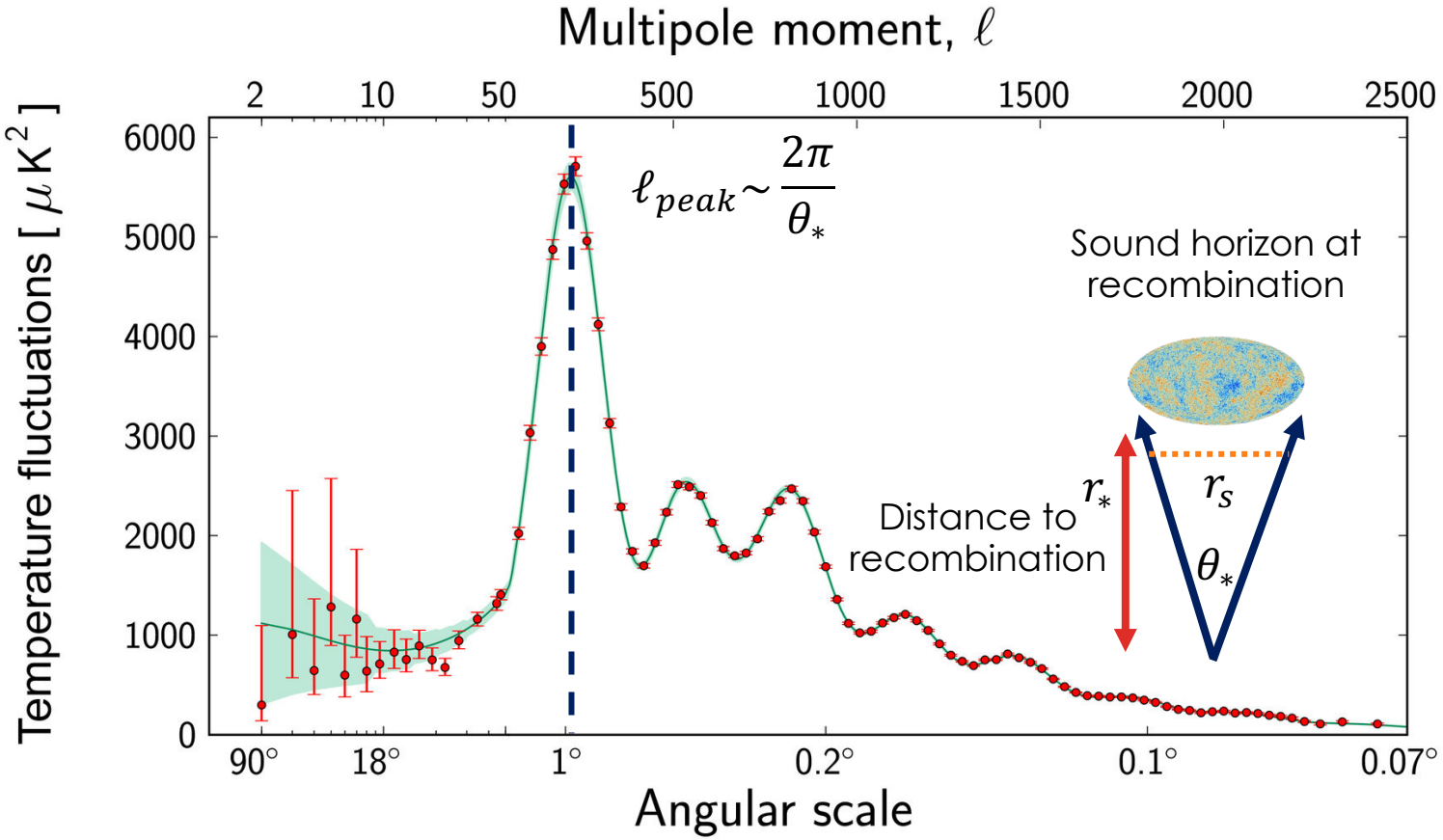

THE HUBBLE TENSION

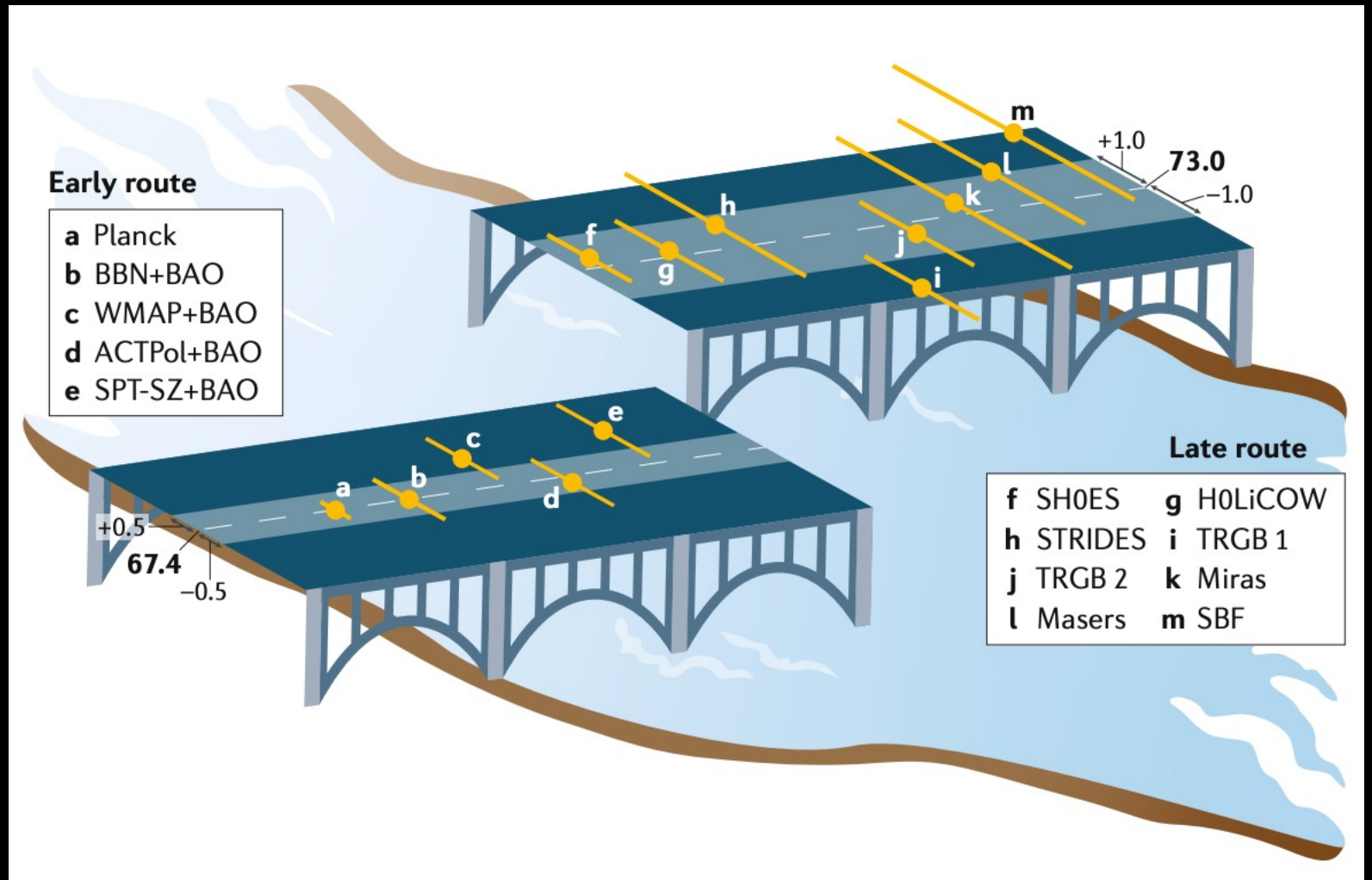

WHAT IS THE HUBBLE TENSION?

- The H0 tension is the most statistically significant disagreement between early-universe and late-universe measurements.

- The tension is about 5σ disagreement between direct measurement of H0 based on standard candles done by SH0ES team and inferred value from CMB observations obtained by Planck team.

- The Planck estimate assuming LCDM model:

$$H_0 = 67.27 \pm 0.60 \frac{km}{sMpc}$$

Planck 2018, Astron. Astrophys. 641 (2020) A6

- The latest local measurements by SH0ES team (R21):

$$H_0 = 73.04 \pm 1.04 \frac{km}{sMpc}$$

Adam G. Riess et al 2022 ApJL ***934*** *L7*

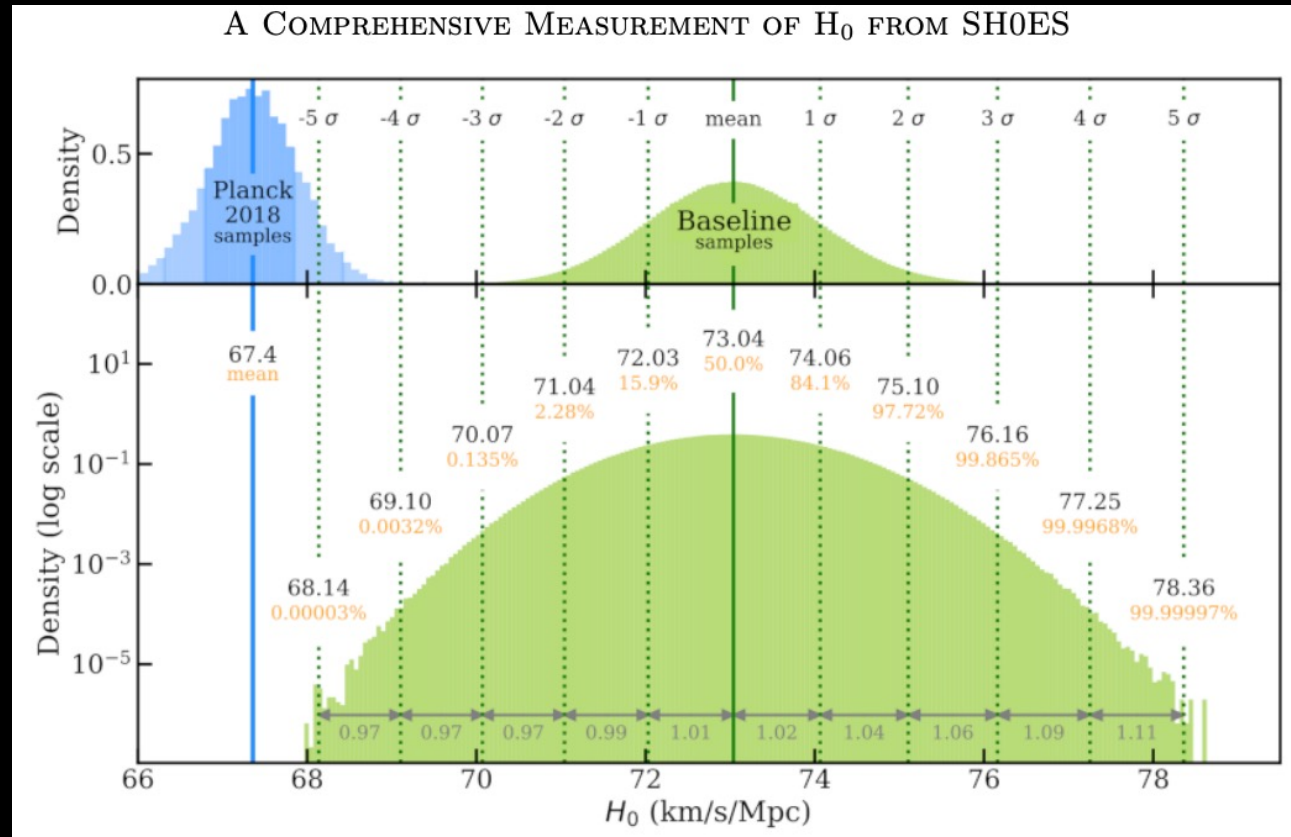

POSSIBLE SOLUTIONS

- Local solution
- Sound horizon problem
- Early Dark Energy
- Late Dark Energy
- Extra relativistic degrees of freedom

  Extra interactions
- Modified gravity
- Inflationary models
- Modified recombination history

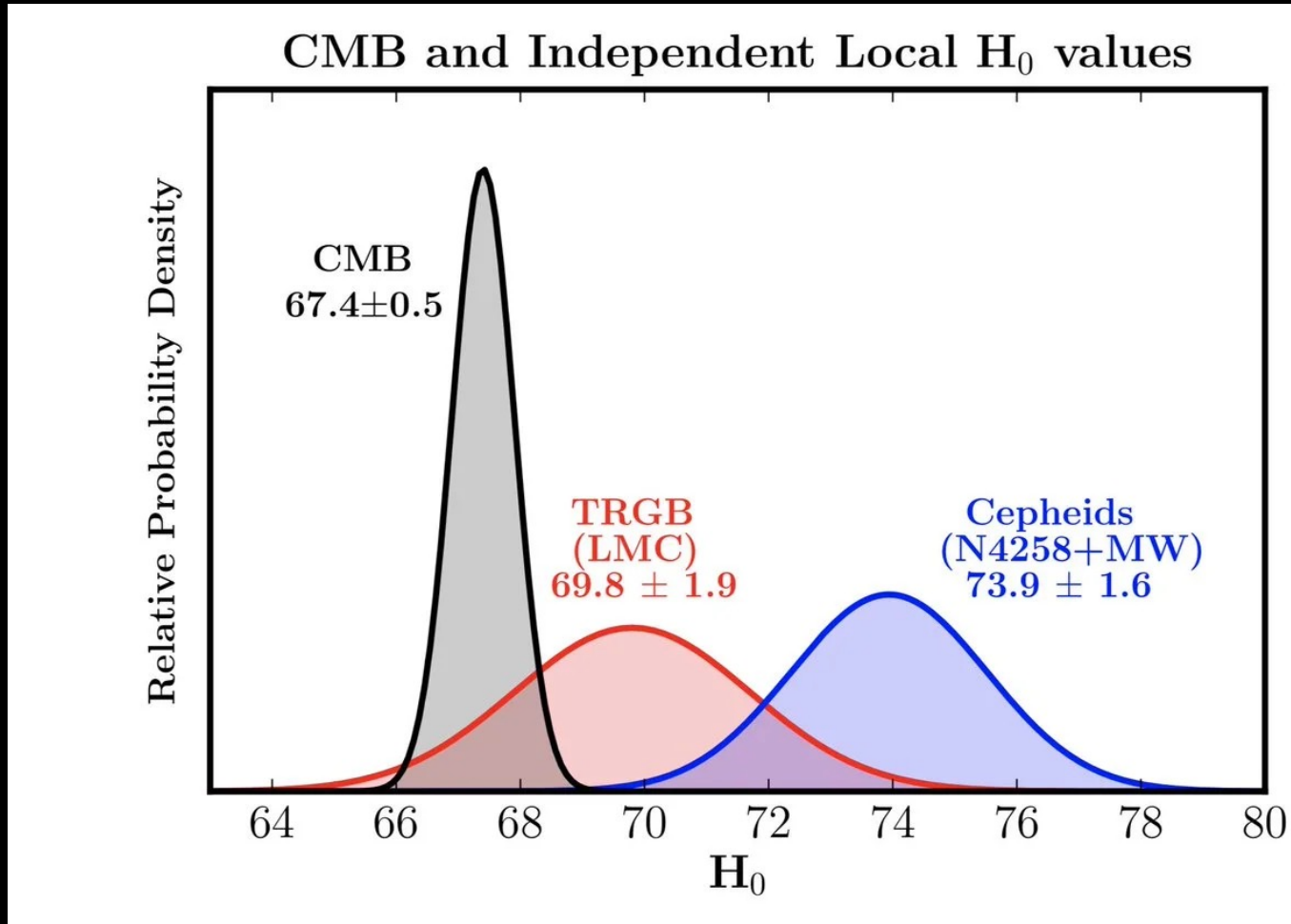

THE THEORY

The Theory

- We consider a model that consists of some new energy density source ρ_x arising from the quantum zero-point energy of the fields with the mass m.
- Depending on the type of the quantum field(boson or fermion) and the energy scale of interest, ρ_x can be either positive (dS-like) or negative (AdS-like).
- For the sake of simplicity, here first we consider the case of a single quantum field, while the procedure for the multiple field is straight forward thanks to our simplifying assumption that the vacuum energies of the free fields do not exchange with each other.

The Theory

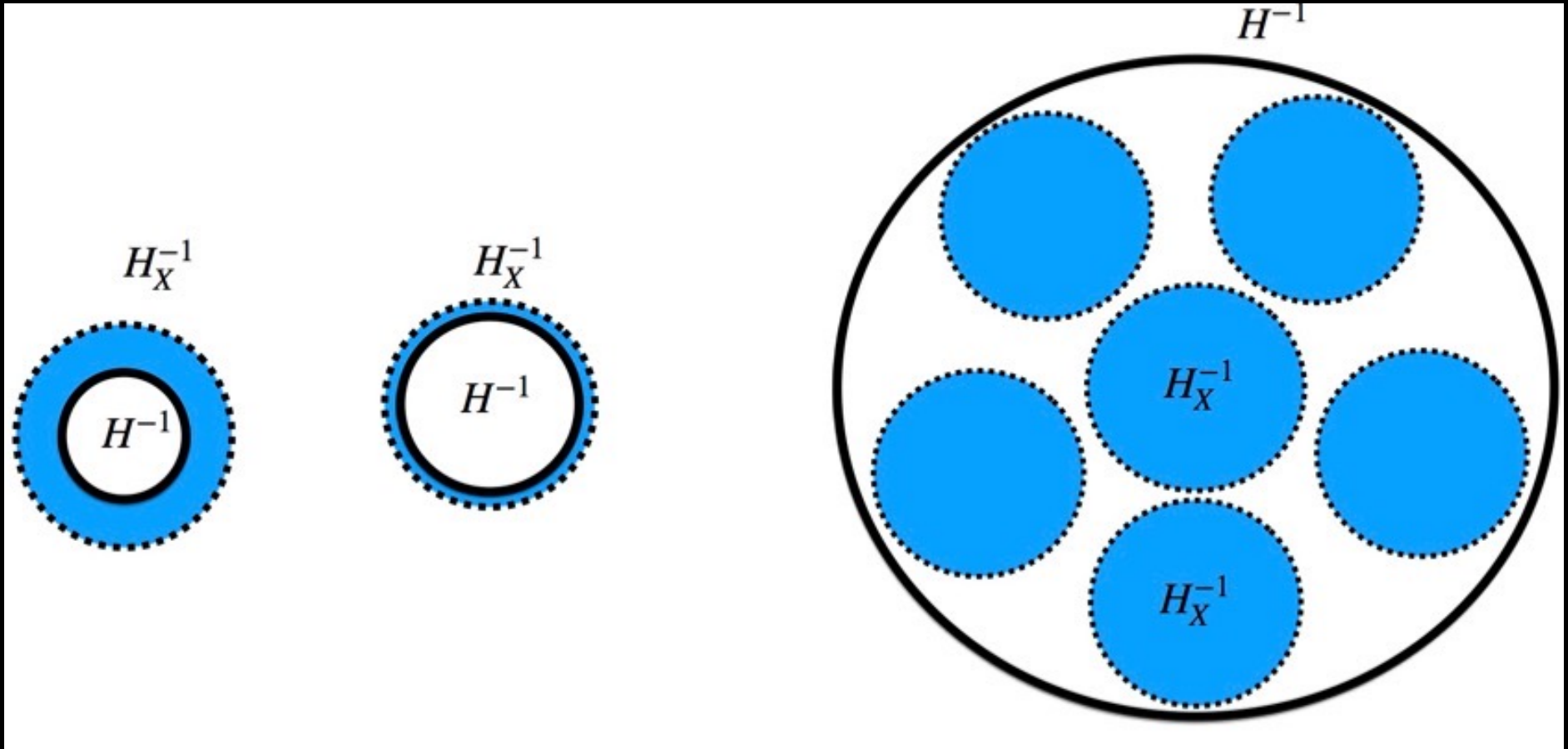

The Theory

- The simplest model satisfying our requirements may be realized by the following ansatz:

$$\rho_X(a) \propto \left[1 + \left(\frac{a}{a_c}\right)^{3(1+w)}\right]^{-1}$$

- With the inclusion of the transfer function:

$$\rho_X(a) = \rho_{X,c}\left[\mathcal{T}(b, a_c - a) + \mathcal{T}(b, a - a_c)\left(\frac{a}{a_c}\right)^{3(1+w)}\right]^{-1}$$

- We consider the following transfer function:

$$\mathcal{T}(b, a - a_c) = \frac{1}{2}[1 + \tanh(b(a - a_c))]$$

The Theory

- We introduce the fraction of dark energy density f_X at the transition scale factor a_c

$$f_X \equiv \frac{\rho_{X,c}}{\rho(a_c)},$$

- The total energy density:

$$\rho(a) = \rho_m\, a^{-3} + \rho_r\, a^{-4} + \rho_\Lambda + \rho_X(a)$$

- At the transition scale:

$$\rho(a_c) = \frac{\rho_m\, a_c^{-3} + \rho_r\, a_c^{-4} + \rho_\Lambda}{1 - f_X}$$

The Theory

- The total energy density of the model is given by

$$\rho(a) = \rho_{\mathrm{m}}\, a^{-3} + \rho_{\mathrm{r}}\, a^{-4} + \rho_{\Lambda} + \frac{\frac{f_X}{1-f_X}(\rho_{\mathrm{m}}\, a_{\mathrm{c}}^{-3} + \rho_{\mathrm{r}}\, a_{\mathrm{c}}^{-4} + \rho_{\Lambda})}{\mathcal{T}(b,\, a_{\mathrm{c}} - a) + \mathcal{T}(b,\, a - a_{\mathrm{c}})\left(\frac{a}{a_{\mathrm{c}}}\right)^{3(1+w)}}.$$

- For the general N-field configuration, yielding to N transitions in dark energy at $a_{c,i}$, we can extend the density to the following form:

$$\rho(a) = \rho_{\mathrm{m},0}\, a^{-3} + \rho_{\mathrm{r},0}\, a^{-4} + \rho_{\Lambda} + \sum_{i=1}^{N} \frac{\frac{f_i}{1-f_i}(\rho_{\mathrm{m}}\, a_{\mathrm{c},i}^{-3} + \rho_{\mathrm{r}}\, a_{\mathrm{c},i}^{-4} + \rho_{\Lambda})}{\mathcal{T}(b_i,\, a_{\mathrm{c},i} - a) + \mathcal{T}(b_i,\, a - a_{\mathrm{c},i})\left(\frac{a}{a_{\mathrm{c},i}}\right)^{3(1+w_i)}}.$$

OBSERVATIONAL DATA & METHOD

- CMB: temperature and polarization angular power spectra from the final release of Planck 2018.
- BAO: 6dFGS, SDSS-MGS, BOSS DR12.
- SN: 1048 SNe Type Ia luminosity distance from the Pantheon sample.

OBSERVATIONAL DATA & METHOD

- To analyze the data and extract the constraints on the cosmological parameters, we have modified the well-known cosmological Markov Chain Monte Carlo package CosmoMC.
- We assumed a convergence diagnostic based on Gelman-Rubin statistic, assuming R-1 < 0.1 .
- The parameter space for different class of models is given by:

$$\boldsymbol{P = \{a_i, f_i, w_i, n_i, \Omega_b h^2, \Omega_{cdm} h^2, 100\,\theta_{MC}, \tau, n_s, A_s\}}$$

ONE-STEP MODELS

One-step models

TESTING DIFFERENT STEP POSITIONS

Priors for One-step Models for Different Step Positions

Parameter	Priors Model 1	Priors Model 2	Priors Model 3
$1 + z_{c,1}$	25	250	2500
f_1	0.20	0.20	0.20
w_1	[0.5, 1]	[0.5, 1]	[0.5, 1]
n_1	[−1, 1.5]	[−1, 1.5]	[−1, 1.5]

One-step models

Testing different step positions

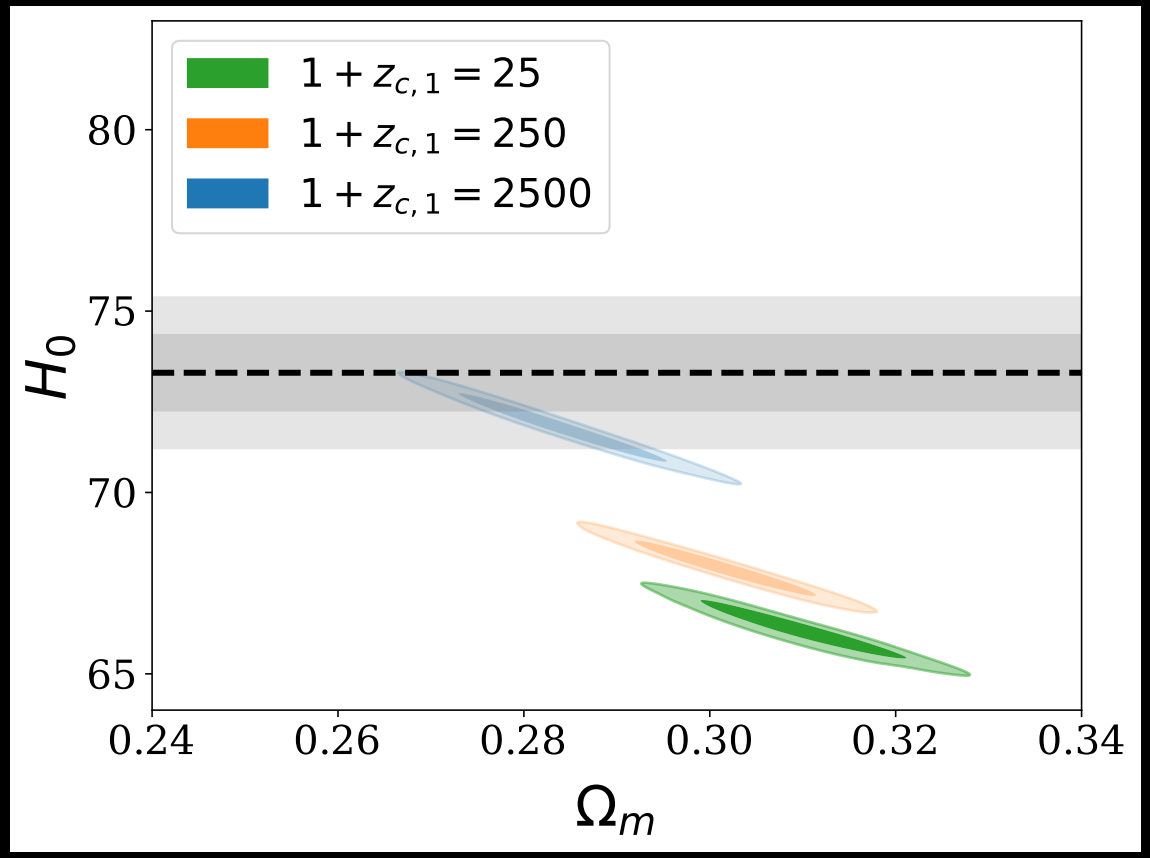

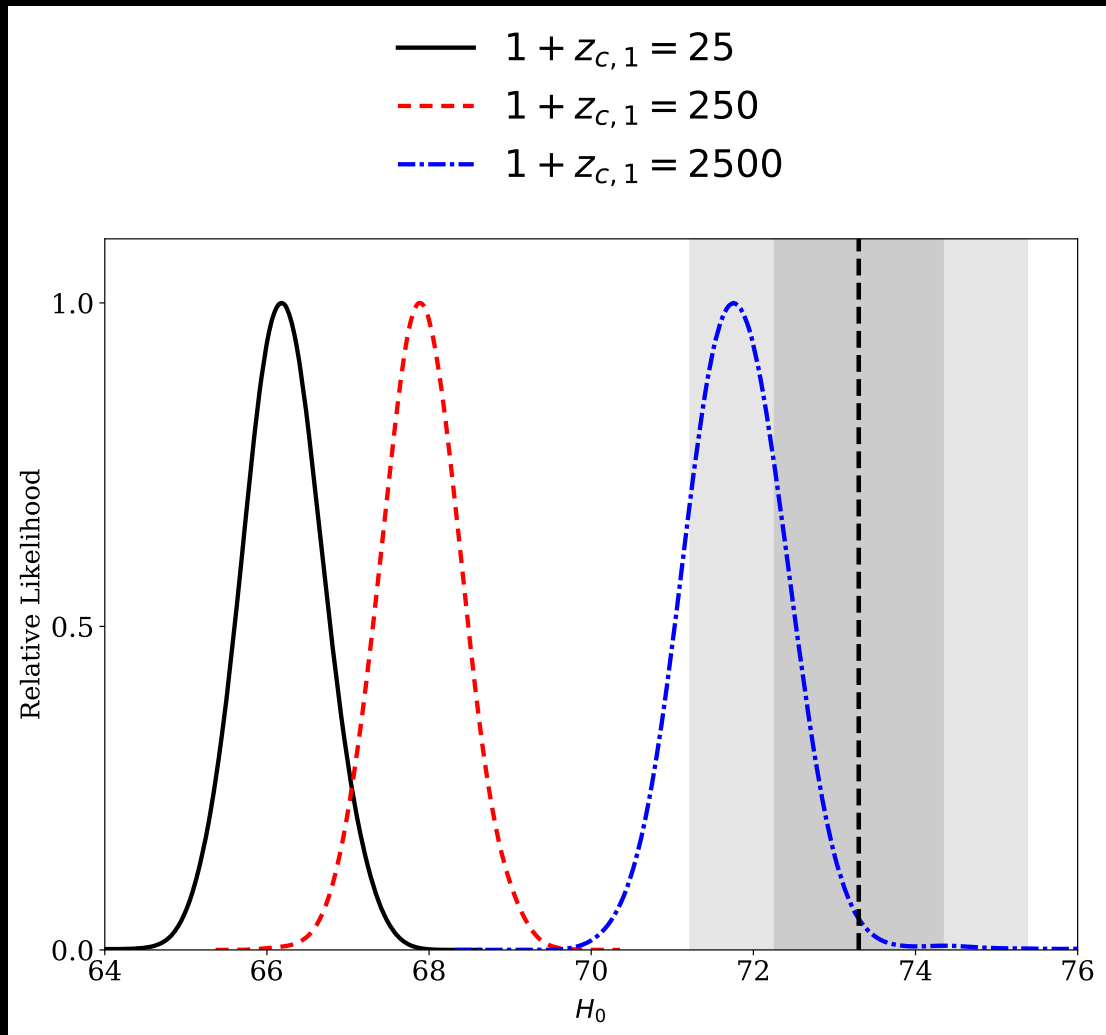

One-step models

TESTING DIFFERENT STEP POSITIONS

The 68% Limits for Parameters of One-step Models Compared to the ΛCDM model

Parameter	Best-fit ΛCDM	Best-fit Model 1	Best-fit Model 2	Best-fit Model 3
n_1	···	>0.945	>1.18	>1.46
w_1	···	>0.880	>0.923	0.808 ± 0.060
Ω_m	0.3092 ± 0.0070	0.3107 ± 0.0073	0.3040 ± 0.0068	0.2838 ± 0.0085
H_0	67.70 ± 0.52	66.43 ± 0.54	67.80 ± 0.52	$71.83^{+0.59}_{-0.67}$
S_8	0.819 ± 0.014	0.793 ± 0.014	$0.803^{+0.013}_{-0.015}$	0.890 ± 0.018
$10^9 A_s$	2.091 ± 0.027	$2.069^{+0.025}_{-0.028}$	2.086 ± 0.027	2.052 ± 0.029
n_s	0.9668 ± 0.0042	0.9795 ± 0.0044	0.9681 ± 0.0042	0.9932 ± 0.0044
τ	0.0541 ± 0.0059	0.0544 ± 0.0058	0.0551 ± 0.0059	0.0425 ± 0.0065
ΔAIC	0.0	24.38	75.55	808.04

One-step models

TESTING THE EFFECT OF FRACTION OF ENERGY DENSITY

Priors for One-step Models for Different f_1 Strengths

Parameter	Priors Model 4	Priors Model 3	Priors Model 5
$1 + z_{c,1}$	2500	2500	2500
f_1	0.15	0.20	0.25
w_1	[0.5, 1]	[0.5, 1]	[0.5, 1]
n_1	[−1, 1.5]	[−1, 1.5]	[−1, 1.5]

One-step models

Testing the effect of fraction of energy density

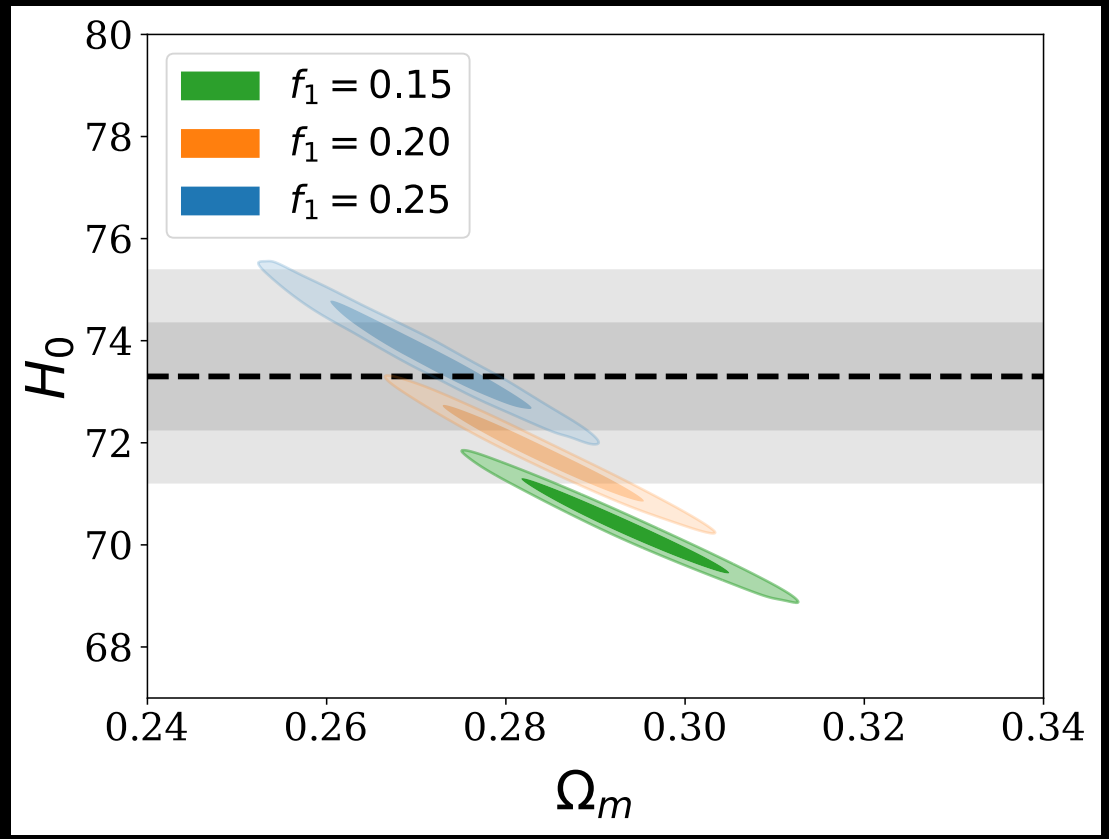

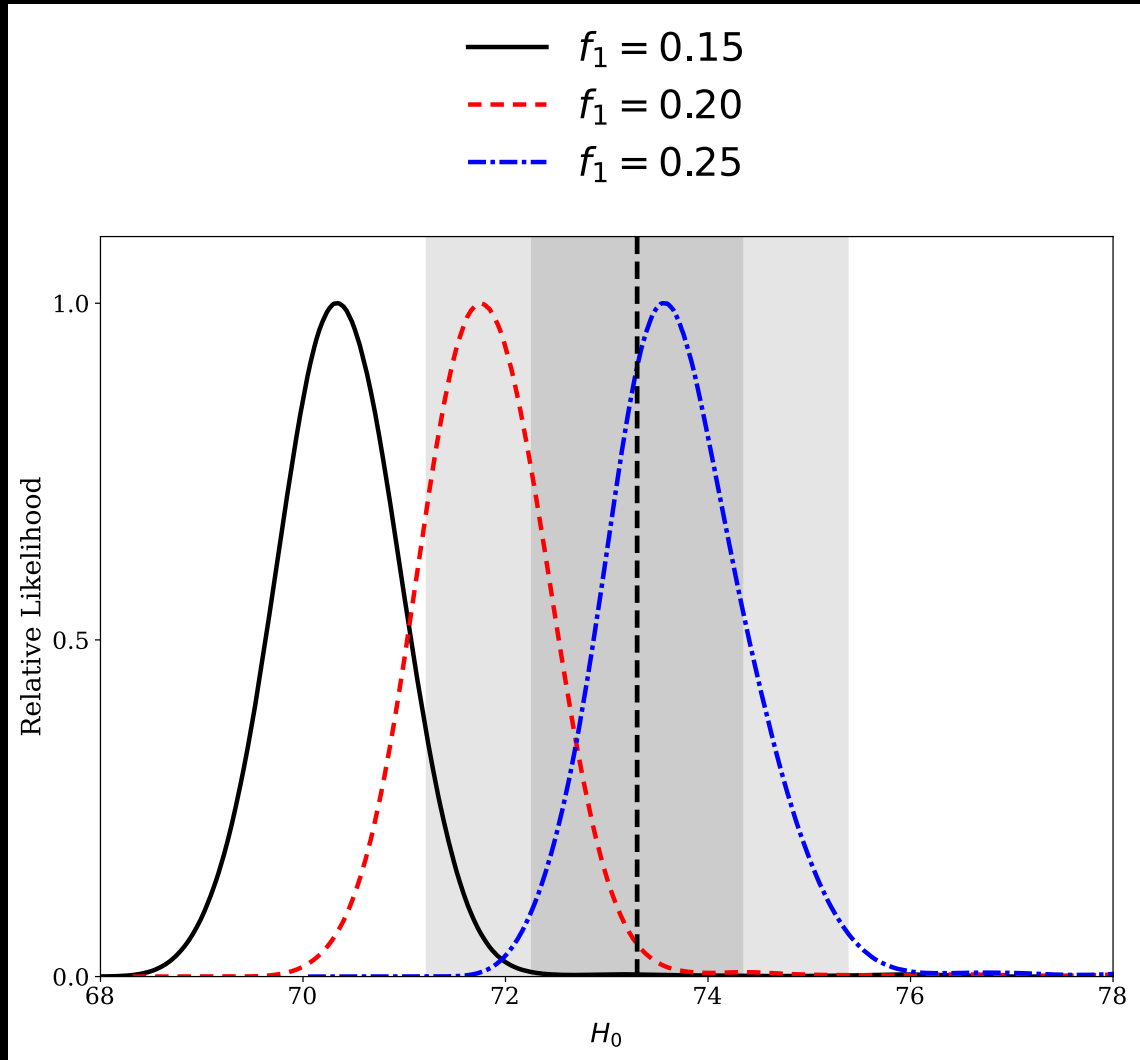

One-step models

Testing the effect of fraction of energy density

Observational Constraints and 68% Limits for One-step Models Based on CMB+BAO+SN Data

Parameter	Best-fit Model 4	Best-fit Model 3	Best-fit Model 5
n_1	>1.42	>1.46	>1.47
w_1	$0.787^{+0.064}_{-0.092}$	0.808 ± 0.060	$0.820^{+0.073}_{-0.032}$
Ω_m	0.2933 ± 0.0080	0.2838 ± 0.0085	$0.2703^{+0.0089}_{-0.0061}$
H_0	70.37 ± 0.68	$71.83^{+0.59}_{-0.67}$	$73.84^{+0.49}_{-0.92}$
S_8	0.873 ± 0.017	0.890 ± 0.018	$0.903^{+0.018}_{-0.014}$
$10^9 A_s$	2.058 ± 0.027	2.052 ± 0.029	2.053 ± 0.030
n_s	0.9815 ± 0.0042	0.9932 ± 0.0044	1.0098 ± 0.0055
τ	0.0449 ± 0.0060	0.0425 ± 0.0065	$0.0414^{+0.0063}_{-0.0077}$
ΔAIC	409.79	808.04	1402.45

Note. The higher the value of f_1, the larger the prediction for H_0.

TWO-STEP MODELS

TWO-STEP MODELS

The effect of second step position

Priors for Two-step Models with Different Second Step Positions $1 + z_{c,2}$

Parameter	Priors Model 6	Priors Model 7	Priors Model 8
$1 + z_{c,1}$	2500	2500	2500
f_1	0.20	0.20	0.20
w_1	[0.5, 1]	[0.5, 1]	[0.5, 1]
n_1	[−1, 1.5]	[−1, 1.5]	[−1, 1.5]
$1 + z_{c,2}$	833	83.3	8.3
f_2	0.10	0.10	0.10
w_2	[0.5, 1]	[0.5, 1]	[0.5, 1]
n_2	[−1, 1.5]	[−1, 1.5]	[−1, 1.5]

Two-step models
The effect of second step position

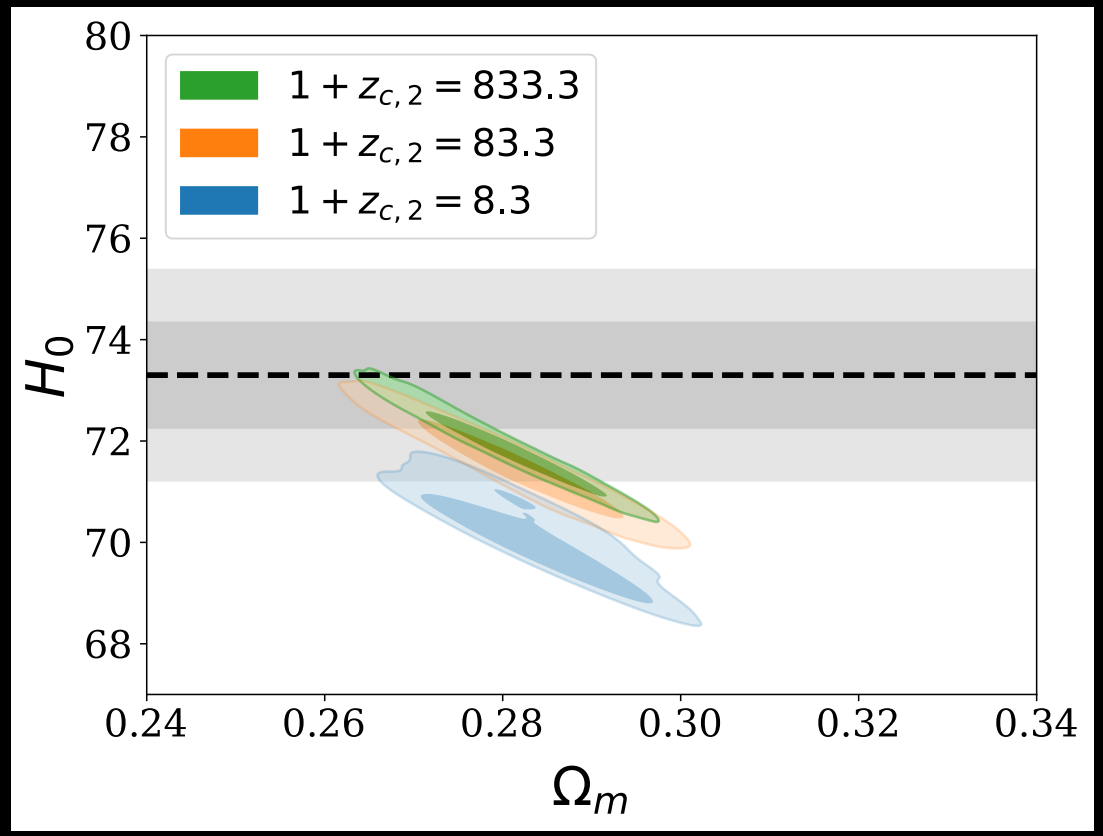

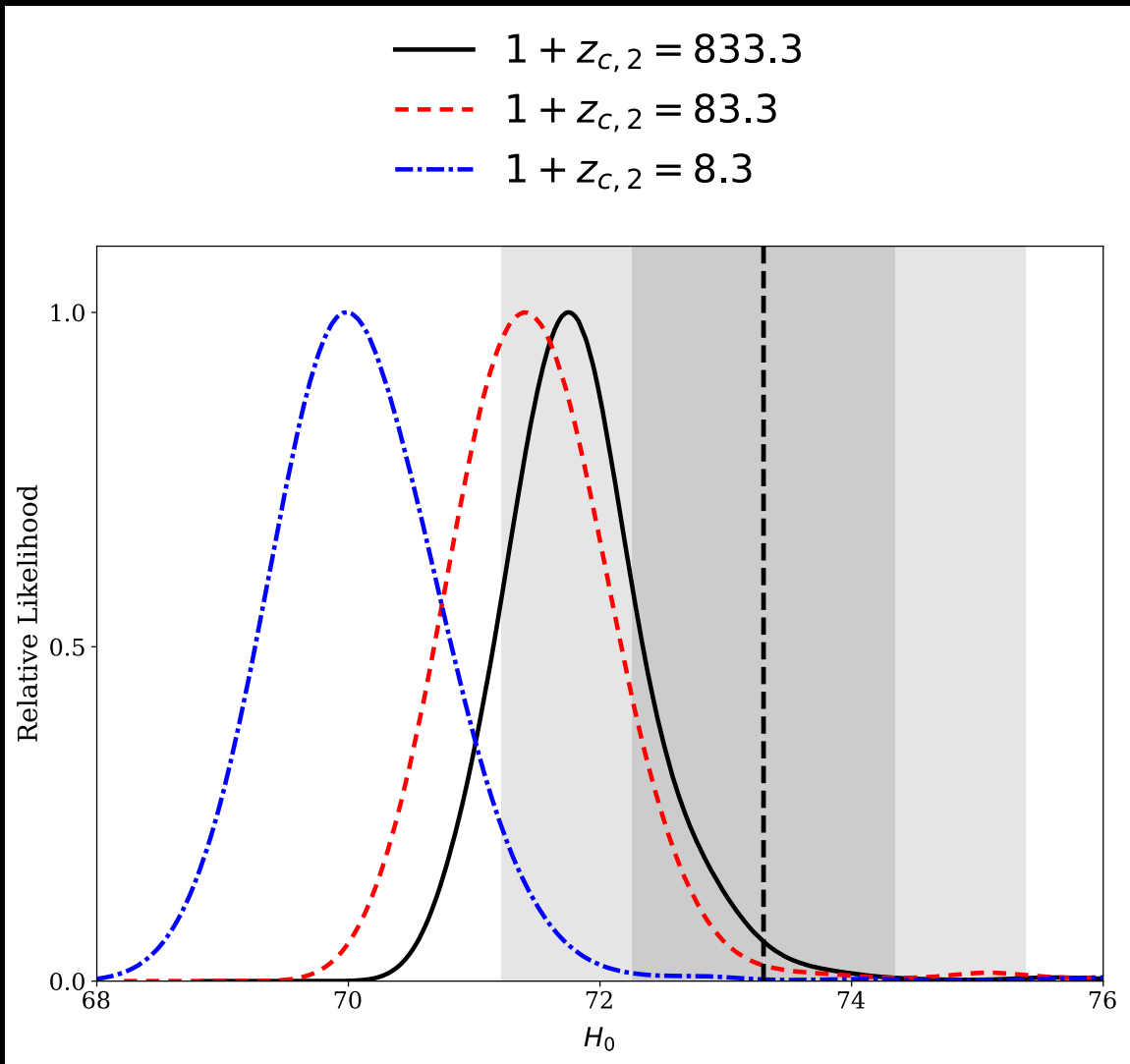

TWO-STEP MODELS

The effect of second step position

The 68% Limits for Parameters of Two-step Models Based on CMB+BAO +SN Data

Parameter	Best-fit Model 6	Best-fit Model 7	Best-fit Model 8
n_1	>1.47	>1.42	>1.46
w_1	>0.984	$0.763^{+0.036}_{-0.057}$	$0.703^{+0.033}_{-0.043}$
n_2	>0.363	...	...
w_2	>0.730	<0.641	<0.576
Ω_m	$0.2801^{+0.0081}_{-0.0055}$	$0.2811^{+0.0085}_{-0.0068}$	0.2832 ± 0.0076
H_0	$71.92^{+0.39}_{-0.74}$	$71.55^{+0.52}_{-0.77}$	$70.11^{+0.59}_{-0.76}$
S_8	$0.876^{+0.017}_{-0.013}$	0.875 ± 0.021	0.853 ± 0.017
$10^9 A_s$	2.019 ± 0.031	$2.039^{+0.025}_{-0.036}$	$2.017^{+0.026}_{-0.030}$
n_s	0.9843 ± 0.0048	$0.9989^{+0.0050}_{-0.0044}$	$1.0085^{+0.0052}_{-0.0044}$
τ	0.0426 ± 0.0072	$0.0434^{+0.0058}_{-0.0078}$	$0.0448^{+0.0056}_{-0.0063}$
ΔAIC	764.35	805.25	764.66

TWO-STEP MODELS

Testing dS or AdS behavior of second step

$f > 0$ **dS**

$f < 0$ **AdS**

Priors for Two-step Models with Opposite Signs of f_2

Parameter	Priors Model 10	Priors Model 11
$1 + z_{c,1}$	2500	2500
f_1	0.25	0.25
w_1	[0.5, 1]	[0.5, 1]
n_1	[−1, 1.5]	[−1, 1.5]
$1 + z_{c,2}$	83.3	83.3
f_2	**dS** 0.15	**AdS** −0.15
w_2	[0.5, 1]	[0.5, 1]
n_2	[−1, 1.5]	[−1, 1.5]

Two-step models

Testing dS or AdS behavior of second step

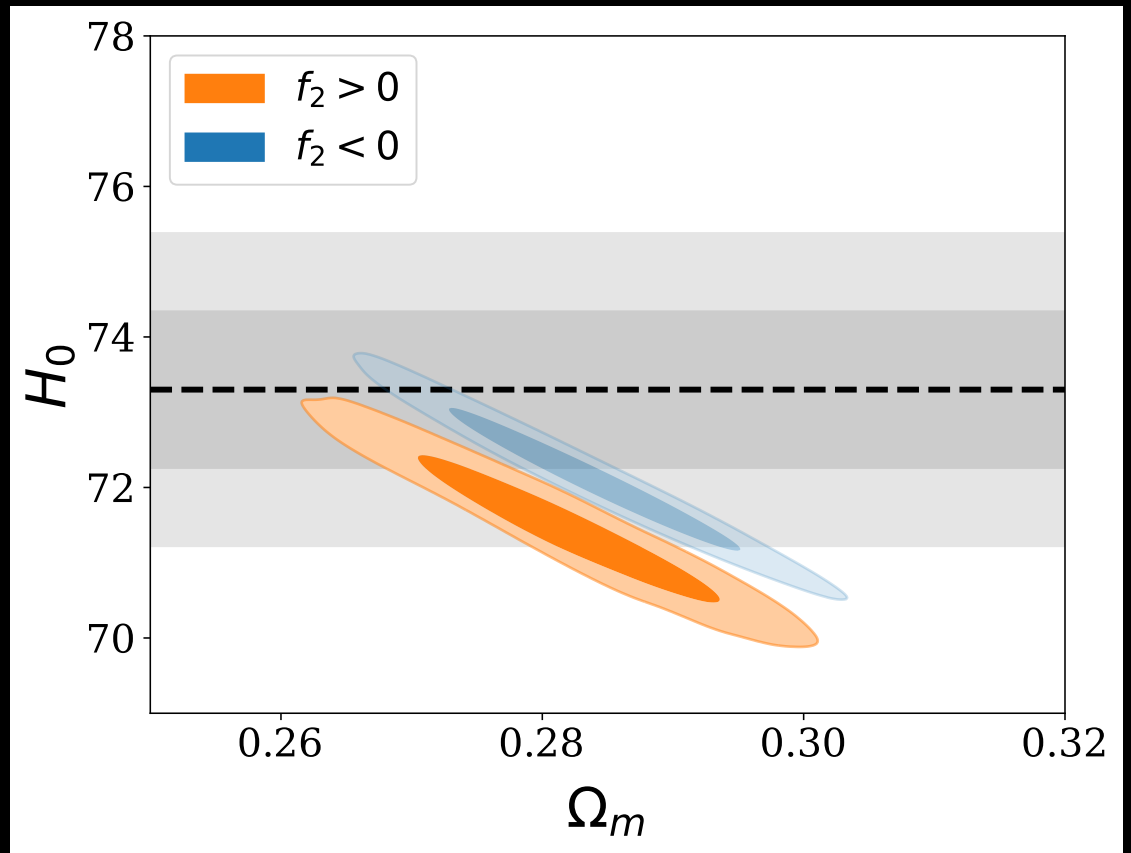

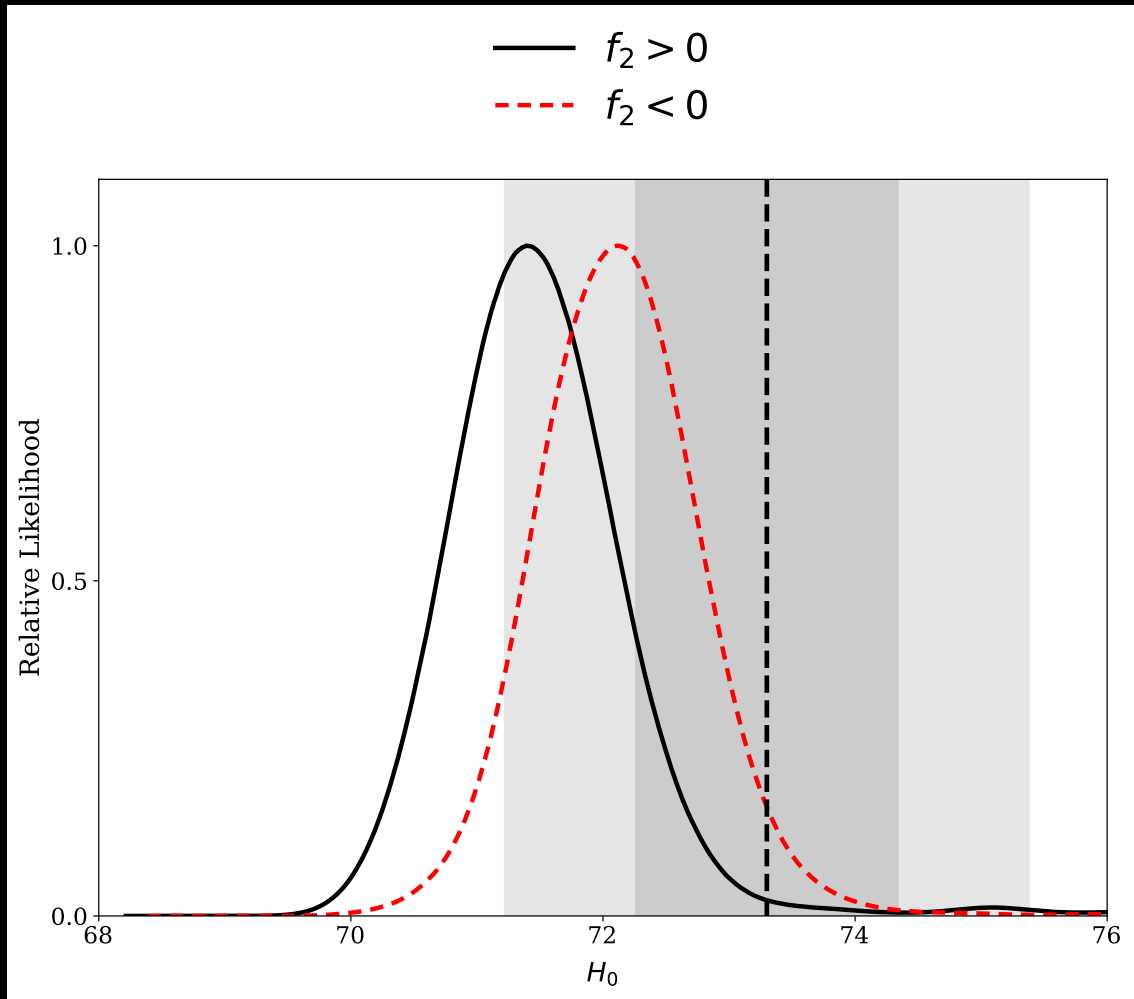

TWO-STEP MODELS

Testing dS or AdS behavior of second step

Summary of Observational Constraints and 68% Limits for Parameters of Two-step Models

Parameter		Best-fit Model 10		Best-fit Model 11
n_1		>1.46		>1.41
w_1		0.762 ± 0.036		$0.824^{+0.087}_{-0.044}$
n_2		<0.957		>1.07
w_2		<0.534		>0.786
Ω_m	dS	$0.2662^{+0.0078}_{-0.0061}$	AdS	$0.267^{+0.011}_{-0.0052}$
H_0		$73.18^{+0.48}_{-0.81}$		$74.70^{+0.34}_{-1.2}$
S_8		$0.875^{+0.017}_{-0.015}$		$0.904^{+0.025}_{-0.013}$
$10^9 A_s$		$2.021^{+0.026}_{-0.032}$		2.060 ± 0.031
n_s		$1.0223^{+0.0054}_{-0.0047}$		1.0077 ± 0.0069
τ		$0.0414^{+0.0059}_{-0.0067}$		$0.0420^{+0.0061}_{-0.0087}$
ΔAIC		1355.95		1453.15

THREE-STEP MODELS

THREE-STEP MODELS

Priors for Three-step Models

Parameter	Priors Model 12	Priors Model 13	Priors Model 14	Priors Model 15
$1 + z_{c,1}$	2500	2500	2500	2500
f_1	0.20	0.20	0.20	0.20
w_1	[0.5, 1]	[0.5, 1]	[0.5, 1]	[0.5, 1]
n_1	[−1, 1.5]	[−1, 1.5]	[−1, 1.5]	[−1, 1.5]
$1 + z_{c,2}$	833	833	833	833
f_2	+0.15	−0.15	+0.15	−0.15
w_2	[0.5, 1]	[0.5, 1]	[0.5, 1]	[0.5, 1]
n_2	[−1, 1.5]	[−1, 1.5]	[−1, 1.5]	[−1, 1.5]
$1 + z_{c,3}$	83.3	83.3	83.3	83.3
f_3	+0.15	+0.15	−0.15	−0.15
w_3	[0.5, 1]	[0.5, 1]	[0.5, 1]	[0.5, 1]
n_3	[−1, 1.5]	[−1, 1.5]	[−1, 1.5]	[−1, 1.5]

Three-step models

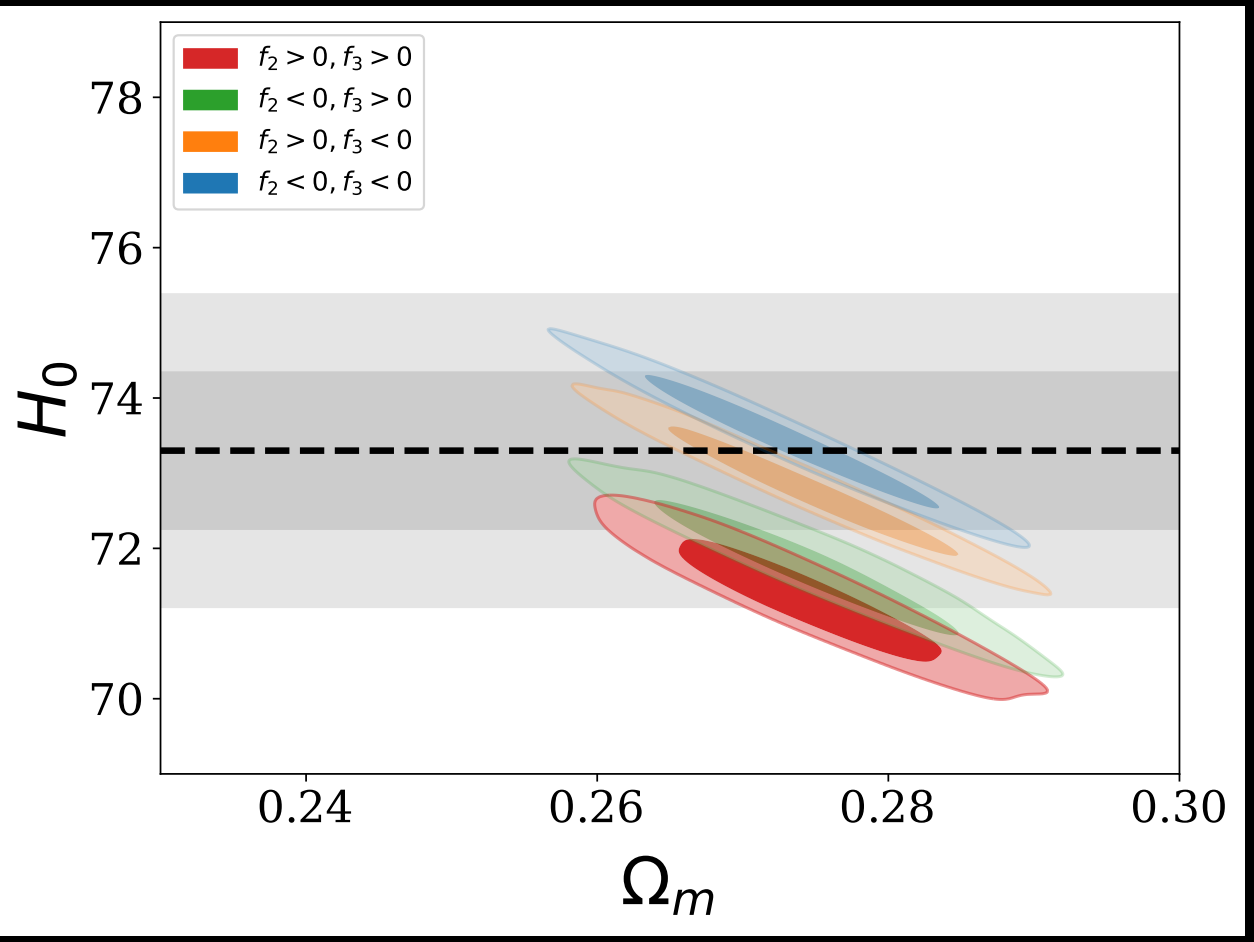

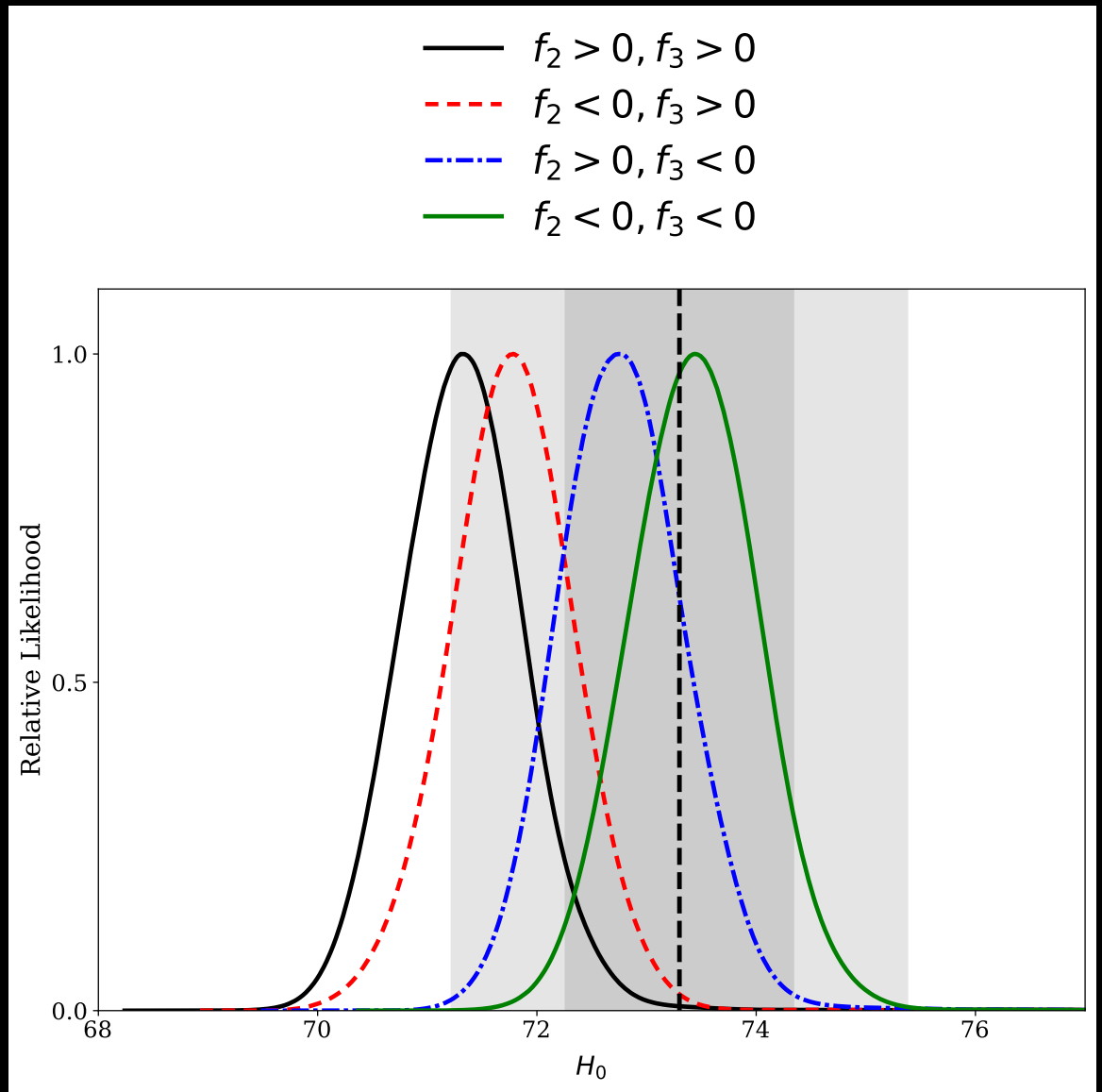

THREE-STEP MODELS

Constraints of 68% Limits and Best-fit Values for Parameters of Three-step Models

Parameter	Best-fit Model 12	Best-fit Model 13	Best-fit Model 14	Best-fit Model 15
n_1	>1.45	>1.44	>1.45	>1.44
w_1	>0.988	<0.511	>0.992	<0.517
n_2	>1.05	>1.11	>1.10	>1.14
w_2	>0.938	>0.842	>0.797	>0.938
n_3	<0.527	<−0.609	>0.514	>0.916
w_3	<0.557	<0.542	>0.844	>0.865
Ω_m	0.2743 ± 0.0068	$0.2746^{+0.0062}_{-0.0069}$	0.2743 ± 0.0076	0.2730 ± 0.0070
H_0	71.35 ± 0.67	71.77 ± 0.59	$72.81^{+0.50}_{-0.64}$	73.46 ± 0.66
S_8	0.845 ± 0.016	0.862 ± 0.017	0.874 ± 0.017	0.892 ± 0.018
$10^9 A_s$	1.977 ± 0.029	$2.030^{+0.025}_{-0.028}$	2.006 ± 0.028	2.062 ± 0.028
n_s	0.9942 ± 0.0046	$1.0197^{+0.0047}_{-0.0041}$	0.9810 ± 0.0043	1.0071 ± 0.0044
τ	0.0430 ± 0.0064	0.0419 ± 0.0059	0.0425 ± 0.0067	0.0422 ± 0.0063
ΔAIC	744.79	836.76	774.85	908.96

CONCLUDING REMARKS

- Our investigations show that the resulting values of H_0 are not sensitive to the locations of the second or third transitions.
- But they are largely sensitive to the values and the signs of the fractions of dark energy, f_2 and f_3.
- Our analysis also shows that to obtain values of H_0 comparable to the value obtained from local measurements requires n_s to move toward the Harrison–Zel'dovich scale-invariant value.
- The least tension in the H_0 value occurs in a Two-step model in which both steps occur in dS-like phases.
- Also least tension occurs in a Three-step model in which its first phase is dS-like and the evolution of the second and third steps occurs in AdS-like phases

"I have deep faith that the principle of the Universe will be beautiful and simple”

- Albert Einstein

THANKS FOR YOUR ATTENTION !